

# Parametrizing confocal parameters for characterizing the optical properties of human brain tissue using high numerical aperture optical coherence tomography

Jiarui Yang<sup>1</sup>, Ichun Anderson Chen<sup>1</sup>, Shuaibin Chang<sup>1</sup>, Jianbo Tang<sup>1</sup>, Blaire Lee<sup>1</sup>, Kivildim Kılıç<sup>1</sup>, Hui Wang<sup>2</sup>, Caroline Magnain<sup>2</sup>, Shih-chi Chen<sup>3</sup>, Bruce Fischl<sup>2</sup>, David A. Boas<sup>1,\*</sup>

<sup>1</sup>Department of Biomedical Engineering, Boston University, Boston, MA, USA

<sup>2</sup>Athinoula A. Martinos Center for Biomedical Imaging, Department of Radiology, Massachusetts General Hospital, MA, USA

<sup>3</sup>Department of Mechanical and Automation Engineering, The Chinese University of Hong Kong, Hong Kong SAR, China  
\*email: dboas@bu.edu

**Abstract:** A systematic method was developed to parametrize confocal parameters for modeling the depth profile of optical coherence tomography images in highly scattering media. This approach enables improved quantification of optical properties of human brain tissue. © 2020 The Author(s)

## 1. Introduction

Optical coherence tomography (OCT) is a volumetric imaging technique that has been widely used to study the microstructure of biological samples. The OCT image signal originates from back-scattered light and provides distinctive sample contrast such as structural landmarks [1], pathological alterations [2], and various physiological indicators [3]. The depth profile of the OCT signal is determined by four factors: the refraction index of the sample, the attenuation coefficient, the back-scattering coefficient, and the numerical aperture (NA) of the focusing optics [4]. The attenuation coefficient, the sum of the absorption and scattering coefficients, is an intrinsic property of the sample, and is independent of optics and the incident power. For low NA OCT systems, where the lateral resolution is typically larger than 10  $\mu\text{m}$  and the confocal parameter ( $2 \times$  Rayleigh range) is comparable to or larger than the imaging depth, a single-scattering exponential model is appropriate to describe signal attenuation versus depth [5, 6]. However, for high NA OCT systems where the lateral resolution reaches a few microns or less, the shape of the axial point spread function (PSF) is coupled with the depth profiles, thus the effect of the confocal parameter cannot be neglected in deriving the optical properties of the sample [6, 7]. Previous work has established a non-linear model to extract four parameters at the same time, but with high inter-parameter correlation, which resulted in large variance and inaccuracy [4]. Here we further developed a systematic approach to parametrize the confocal parameters across a 3D OCT image to further constrain and reduce the degrees of freedom in the non-linear coefficient fitting problem, resulting in improved confidence in the estimated optical properties of the sample.

## 2. Methods

Due to the shallow depth range we want to image in fixed ex-vivo brain, we assume that multiple scattered light has negligible contribution to the detected signal. Based on Schmitt [6] and Izatt [7], the derived depth dependent single scattering model of the OCT signal can be written as:  $A(z) = \frac{\eta e \tau_i P_0}{2h\nu} \sqrt{R(z)}$  (1), where  $P_0$  is the incident power,  $\eta$  is the quantum efficiency of the sensor,  $e$  is the electron charge,  $\tau_i$  is the integration time of the camera, and  $h\nu$  is the photon energy.  $R(z)$  is the reflectance from the sample at the depth of  $z$ . In the near-infrared range, light attenuation within the tissue is dominated by scattering and light absorption is negligible. Therefore, we use the scattering coefficient ( $\mu_s$ ) to approximate the total attenuation coefficient. The depth profile for the OCT signal could be expressed as:  $R(z) = \mu_b \cdot \exp(-2\mu_s z) \cdot h(z)$  (2), where  $h(z)$  is the axial PSF, which is dependent on the refractive index of the medium ( $n$ ), the focus depth ( $z_f$ ) and the Rayleigh range ( $z_r$ ). In a single mode fiber based OCT system, the light beam in the sample arm approximately follows a Gaussian distribution [8]. We use a simplified PSF model that neglects the effect of a refractive index difference at the tissue-water interface:  $h(z) = \frac{1}{1 + (\frac{z-z_f}{n z_r})^2}$  (3). Furthermore,

$z_r$  can be calculated from the beam waist at the focus, center wavelength of the laser and the NA of the optics. However, in highly scattering medium, the effective Rayleigh range ( $z'_r$ ) has been shown to also vary as a function of  $z_f$  and  $\mu_s$  [9]:  $z'_r = z_r + \frac{\lambda_0 z_f \mu_s}{4n\pi}$  (4).

We observed that  $z_f$  was almost horizontal in liquid phantoms after field curvature correction, which suggests  $z_f$  variation in human brain sample was mostly caused by the slope between the sample surface and image plane. Thus, a linear plane was empirically fitted to represent  $z_f$  within the field of view (FOV):  $z_f(x, y) = A + Bx + Cy$  (5), where  $x$  and  $y$  correspond to positions in FOV. To implement our model in agarose-embedded human brain samples,

we first extracted linear coefficients in equation (5) using agarose tiles to characterize  $z_f$  within each FOV, then the constant term was estimated for each FOV based on the averaged depth profile across the entire FOV to reflect the global change in sample surface. Once  $z_f$  is known,  $z'_r$  was further parametrized as a parabolic surface as a function of  $\mu_s$ , which reduced the degrees of freedom of the confocal parameters in our model.

Finally, we adopted a previously introduced relative back-scattering coefficient  $\mu'_b = \left(\frac{\eta e \tau_i P_0}{2 h \nu}\right)^2 \mu_b$  to further simplify our fitting model. This coefficient could be used to estimate the relative changes in  $\mu_b$  [4].

All measurements were performed on a spectral domain OCT system (Thorlabs, New Jersey). The light source is a broadband super luminescent diode with center wavelength of 1300 nm and bandwidth of 150 nm. A 10x air objective (Mitutoyo) with a z spacer was used in the sample arm, which yields to a lateral resolution of 3.5  $\mu\text{m}$  with a theoretical Rayleigh range of 40  $\mu\text{m}$  in a non-scattering medium.

A block of human brain was obtained from the Massachusetts General Hospital Autopsy Suite. The brain sample was fixed with 10% formalin for at least two months. The postmortem interval did not exceed 24 h. The block was embedded in oxidized agarose and covalently cross-linked with the agarose using borohydride borate solution. The surface of the embedded sample was flattened using a vibratome slicer before OCT imaging [10].

### 3. Results

We report the implementation of the parametrization routine to extract the optical properties of human brain tissue. The volumetric imaging spanned a FOV of 1 x 1 x 2.6  $\text{mm}^3$ , with a voxel size of 2.5 x 2.5 x 2.6  $\mu\text{m}^3$ . There was a 50% overlap between adjacent tiles to ensure reliable registration and uniform speckle reduction. Motorized xyz stages were integrated under the sample arm to automatically translate the sample between image tiles. The whole section was imaged in 576 tiles. We used Fiji software to stitch the tiles and create the mosaic images [11]. To compare with conventional OCT contrast, we computed the averaged intensity projection (AIP) within 250  $\mu\text{m}$  depth range starting from 35  $\mu\text{m}$  below the tissue surface in order to reduce the impact of specular reflection from the surface. We then used the same depth range data to fit both the full four-parameter model and our parametrized model. After parametrization, additional features, such as vessels and fiber bundles were recovered. A set of intralipid liquid phantoms was prepared to create different levels of scattering that is comparable to human brain. Both full model and parametrized model were able to extract  $\mu_s$  of the phantoms. However, the standard deviation of  $\mu_s$  within a 1  $\text{mm}^2$  FOV was smaller in the parametrized model, which suggests more consistent quantification of optical properties.

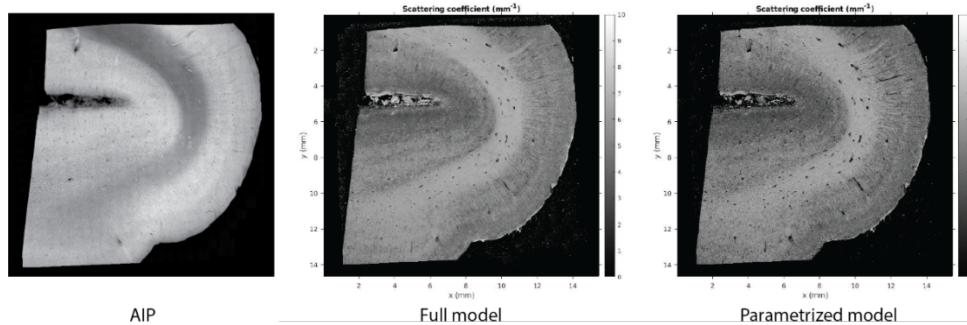


Figure 1: Left: AIP image. Middle: extracted  $\mu_s$  using full model. Right: extracted  $\mu_s$  using parametrized model.

### 4. References

- [1] Hee, M. R., et al., Optical coherence tomography of the human retina. *Archives of ophthalmology*, 1995. 113(3), 325-332.
- [2] Brezinski, M. E., et al., Optical coherence tomography for optical biopsy: properties and demonstration of vascular pathology. *Circulation*, 1996. 93(6), 1206-1213.
- [3] Puliafito, C. A., et al., Imaging of macular diseases with optical coherence tomography. *Ophthalmology*, 1995. 102(2), 217-229.
- [4] Wang, H., et al., Characterizing the optical properties of human brain tissue with high numerical aperture optical coherence tomography. *Biomedical optics express*, 2017. 8(12): p. 5617-5636.
- [5] Xu, C., et al., Characterization of atherosclerosis plaques by measuring both backscattering and attenuation coefficients in optical coherence tomography. *Journal of biomedical optics*, 2008. 13(3): p. 034003.
- [6] Schmitt, J.M., et al., Optical characterization of dense tissues using low-coherence interferometry. in *Holography, Interferometry, and Optical Pattern Recognition in Biomedicine III*. 1993. International Society for Optics and Photonics.
- [7] Izatt, J.A., et al., Optical coherence microscopy in scattering media. *Optics letters*, 1994. 19(8): p. 590-592.
- [8] van Leeuwen, T.G., et al., Measurement of the axial point spread function in scattering media using single-mode fiber-based optical coherence tomography. *IEEE Journal of selected topics in quantum electronics*, 2003. 9(2): p. 227-233.
- [9] Theer, P. and W. Denk, On the fundamental imaging-depth limit in two-photon microscopy. *JOSA A*, 2006. 23(12): p. 3139-3149.
- [10] Ragan, T., et al., Serial two-photon tomography for automated ex vivo mouse brain imaging. *Nature methods*, 2012. 9(3): p. 255.
- [11] Preibisch S, et al., Globally optimal stitching of tiled 3D microscopic image acquisitions. *Bioinformatics*, 2009, 25(11): p. 1463-1465.

### Acknowledgement

This research is supported by the NIH Brain Initiative Cell Census Network U01 MH117023.